Malaysian Journal of Chemistry, 2026, Vol. 28(4), 172-183

Development of Eco-Friendly Synthetic Leather Utilizing Sugarcane Bagasse Ash as a Filler

Nur Mutia Rosiati[1]*, Fitrilia Silvianti[2], Nunik Purwaningsih[3], Galuh Puspita Sari[3], Diana Ross Arief[2], Ahmat Nuryanto[2], Wikan Berliana Dewi[2] and Yesi Pradika Sari[2]

[1]Department of Leather Processing Technology, Politeknik ATK Yogyakarta, Sewon, Bantul 55281, Indonesia

[2]Department of Rubber and Plastic Processing Technology, Politeknik ATK Yogyakarta, Sewon, Bantul 55281, Indonesia

[3]Department of Leather Product Processing Technology, Politeknik ATK Yogyakarta, Sewon, Bantul 55281, Indonesia

*Corresponding author (e-mail: mutiarosiati@atk.ac.id)

Filler materials are essential as auxiliary components in enhancing the mechanical properties and heat resistance of synthetic leather. The most commonly used filler, $CaCO_3$, often shows poor performance due to weak interfacial interactions with the polymer matrix, prompting the development of alternative fillers. In this study, sugarcane bagasse ash (SBA), a waste product rich in silica, was explored as a potential auxiliary filler for synthetic leather. The use of SBA as an alternative filler in synthetic leather is still limited and requires further investigation. SBA not only improves leather quality but also supports sustainability by repurposing waste and reducing the environmental impact of synthetic leather production. This study investigated the effect of varying SBA content on the properties of synthetic leather. Different amounts of SBA (0%, 20%, 40%, 60%, 80%, and 100%) were incorporated into leather samples to evaluate its impact on the material's properties. The resulting samples were assessed through visual inspection, physical testing using a Universal Testing Machine (UTM), and chemical analyses using a Fourier Transform Infrared (FTIR) spectrophotometer, Scanning Electron Microscope-Energy Dispersive X-ray (SEM-EDX), X-ray diffractometer (XRD), and Thermal Gravimetric Analyser (TGA). The results revealed that 60% SBA content (S-60) achieved the best performance, demonstrating superior thermal stability, tensile strength, and tear strength. The S-60 sample showed a quality comparable to commercial products, with maximum tensile and tear force values of 410.74 N and 57.91 N, respectively.

Keywords: Synthetic leather, sugarcane bagasse ash, silica, filler

Received: March 2026; Accepted: June 2026

Synthetic leather is a substitute material for natural leather in the manufacture of leather products such as shoes and upholstery [1]. Synthetic leather can be produced using polyvinyl chloride (PVC) or polyurethane (PU) as the top layer and fabric as the reinforcing layer. The raw materials that are commonly used are flexible, such as plastic and rubber. Generally, three materials are used in producing synthetic leather, namely the main composition (resin), solvent, and auxiliary material.

Auxiliary materials used for making synthetic leather include plasticizers, stabilizers, fillers, and colouring agents. Fillers serve to reduce polymer production costs, speed up the moulding process, and increase the thermal conductivity of polymers [2]. In addition, a filler also serves to improve the material's mechanical properties, especially the Young modulus and stress values of the composite, provided that good dispersion and strong interfacial interaction between the filler and matrix are achieved [3, 4]. Thus, fillers play an important role in synthetic leather as they simultaneously improve mechanical properties and processing efficiency while reducing material costs.

Various types of fillers can be used to achieve these aims, such as lime ($CaCO_3$), clay, alumina trihydrate (ATH), kaolin, talc, and metal oxides [5–11]. However, the use of $CaCO_3$ as a filler results in weak interfacial interactions with the polymer matrix, thereby limiting its effectiveness in enhancing material properties [12]. Consequently, alternative fillers are required. Several metal oxides are known to prevent the emission of HCl gas during the recycling process of synthetic leather products, making it more environmentally friendly [13]. Metal oxides as fillers can be obtained from several sources, such as bagasse ash. Bagasse ash contains silica (SiO_2), alumina (Al_2O_3), iron oxide (Fe_2O_3), calcium oxide (CaO), and other metal oxides in smaller amounts [14–17]. The dominant metal oxide contained in bagasse ash is silica [15–17]. Silica is well-known as a major

component of Portland cement and plays a vital role in strength development. This is attributed to its ability to promote strong synergistic interactions among the constituents of the material, leading to improved mechanical properties [18]. This behaviour, known as pozzolanic activity, is also exhibited by bagasse ash and has been proven to enhance the mechanical strength and durability of concrete [15, 16, 19]. Therefore, bagasse ash as an auxiliary material for improving the mechanical properties of the composite has been an interesting subject for researchers [20, 21].

Sugarcane bagasse ash (SBA) is a waste from the sugar production process, which is considered useless and destructive to soil fertility. However, bagasse ash has appeared as a new alternative filler for synthetic leather because it contains 38.23% to 98.40% silica [22, 23]. In addition, bagasse ash as a cellulosic waste has many other potential uses, including as a reinforcing material and a composite material [24–27]. Therefore, processed bagasse waste has the potential to reduce environmental pollution [28]. Currently, the application of SBA as an alternative filler in synthetic leather has not been widely investigated. This study aims to determine the effect of adding bagasse ash to synthetic leather products to improve their physical properties and thermal resistance.

EXPERIMENTAL

Materials

SBA was obtained from a sugarcane mill in Madiun, East Java, Indonesia. Materials used included polyvinyl chloride (PVC), dioctyl phthalate (DOP) as a plasticizer, a heat stabilizer (Lastab), epoxy as an adhesive, and knit fabric as a reinforcement material. All chemicals were of industrial grade and used without further purification. Commercial PVC-based synthetic leather X and Y were used as comparative materials in the analyses.

Preparation of Sugarcane Bagasse Ash

SBA was milled to obtain a particle size of approximately 50 mm. The powder obtained was dried in an oven at 150 °C for 20 min to remove the water content.

Preparation of Eco-friendly Synthetic Leather

The formulation of each composite is given in Table 1. SBA content was varied at 0% (S-0), 20% (S-20), 40% (S-40), 60% (S-60), 80% (S-80), and 100% (S-100). Compounding was conducted by weighing all ingredients and then putting them into a stainless steel container. It was stirred until homogeneous using a mixer, by adjusting the speed from 200 to 1000 rpm for 5 min. The skin compound was then smeared on release paper that was heated in an oven at 190 °C for 10 seconds and adjusted using a feeler gauge of 0.3 mm on the coating table. After that, the skin compound was flattened with a manual roller. The compound was heated in an oven at 200 °C for 30 s.

The heated skin was placed on the coating table to apply adhesive. The thickness of the adhesive applied was adjusted to 0.1 mm. Then, the reinforcing cloth was flattened onto the adhesive surface that had been applied. This was dried in an oven at 190-200 °C for 60 seconds. The dried synthetic leather sheet was cooled at room temperature. Subsequently, the sheet was separated from the release paper and then characterized.

Table 1. Formulation of synthetic leather samples.

Sample Code	SBA (%)	Ingredients (g)				
		PVC Resin	DOP	Heat Stabilizer	Epoxy	SBA
S-0	0	100	40	2	3	0
S-20	20	100	48	2	3	16
S-40	40	100	56	2	3	32
S-60	60	100	64	2	3	48
S-80	80	100	72	2	3	64
S-100	100	100	80	2	3	80

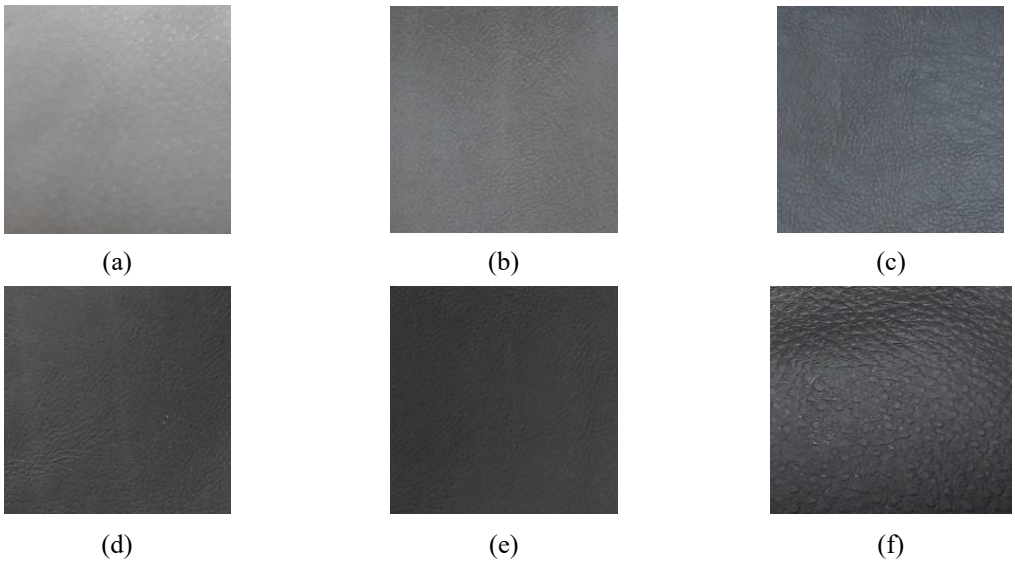

Figure 1. Visual appearance of the synthetic leather samples: (a) S-0, (b) S-20, (c) S-40, (d) S-60, (e) S-80, and (f) S-100.

Characterization techniques

A visual inspection was performed to observe the condition and appearance of the synthetic leather samples. Characterization of materials was conducted using a Universal Testing Machine (UTM) to measure the tensile strength and elongation (SNI 1294:2009). Fourier Transform Infrared (FTIR) spectrophotometry (Shimadzu FTIR Prestige 21), and Scanning Electron Microscopy-Energy Dispersive X-ray (SEM-EDX) (SNE-4500M) were used to identify the functional groups, topography, and elemental content. X-ray diffraction (XRD) (Rigaku Multiflex) analysis was conducted over a 2θ range of 10-40° at a scan speed of 5°/min to evaluate the crystallinity of the material. Thermal Gravimetric Analysis (TGA) (Diamond Pyris Perkin Elmer) was performed to determine the thermal resistance of the synthetic leather composite. The thermal analysis was carried out using a maximum of 4 mg of each sample under a nitrogen gas flow (50 mL/min), with a heating rate of 10 °C/min within the temperature range of 30-1000 °C.

RESULTS AND DISCUSSION

Visual Inspection

A visual inspection was carried out to identify whether the condition and appearance of the eco-friendly synthetic leather samples met the requirements of the Indonesian National Standard (*Standar Nasional Indonesia*, SNI) 1294-2009, a standard for synthetic leather. The quality requirements of this standard include a study of bubbles, wrinkles, cracks, peeling layers, tears, blemishes, and foreign matter attached to materials for determining the goodness or defects of leather. Figure 1 shows the visual appearance of the synthetic leather samples. None of the aforementioned defects were observed in the samples. The sample without SBA produced white coloured synthetic leather. The sugarcane bagasse ash was originally coloured black [29], so the more SBA used, the darker the leather produced. Compounds with more SBA produced black leather. This phenomenon is attributed to the inherent dark colour of SBA, which influences the visual appearance of the synthetic leather [30].

Physical Analysis

Physical parameters including thickness, tensile strength, elongation, tear resistance, and adhesive resistance were measured to explain the effect of SBA as a filler, in reference to SNI 1294-2009. The results of the analysis are shown in Table 2.

Based on Table 2, all the synthetic leather samples met the requirements of SNI, except for S-0, which did not meet the requirements for thickness and maximum tear force. This can be attributed to the absence of a filler, which causes the synthetic leather to become thinner and more susceptible to being torn. However, the thickness of S-80 also did not meet the standard requirements, although it had a higher tear strength than that of S-0. This phenomenon may be a consequence of the compact structure of S-80.

Table 2. Physical properties of the synthetic leather samples.

Material	Thickness (mm)	Maximum Tensile Force (N)	Elongation (%)	Maximum Tear Force (N)	Adhesive Resistance (N)
S-0	0.78	343.23	16.44	14.87	26.22
S-20	0.90	367.04	18.16	47.04	22.89
S-40	0.98	357.37	17.29	53.33	37.32
S-60	0.90	410.74	16.70	57.91	18.17
S-80	0.76	406.30	16.37	47.33	18.71
S-100	0.80	270.67	16.80	51.04	22.31
SNI 1294-2009	Min 0.8	Min 180	12-20	Min 31	Min 14

The best physical properties were obtained with 60% SBA (S-60), and this sample had the highest tensile strength and tear strength values. Its elongation and adhesive resistance values were not the highest observed, but they still exceeded the minimum requirements of SNI. This follows the hypothesis that SBA can improve the physical properties of polymers [29, 31].

With more than 60% of SBA, a decrease in the value of physical parameters was observed, particularly in tensile and tear strength (Table 2). This is because the amount of filler exceeded the ideal composition for polymer composites. The more filler material is added, the more concentrated the polymer compound mixture becomes. If SBA exceeds 80% of the filler material, the composite may exhibit agglomeration or inadequate dispersion, leading to a reduction in mechanical properties [32]. This decrease is attributed to the formation of defects and voids at the SBA-PVC interface, which impair effective load transfer [3]. It has also been noted that the amount of inorganic fillers used can affect the material's physical properties [33, 34].

As a comparison, the physical properties of two commercial synthetic leathers were tested. The results showed that the composite with bagasse ash as filler, especially at 60%, had better physical qualities than the two commercial products in almost all parameters, except adhesive resistance (Table 3.). It can thus be concluded that the quality of the synthetic leather produced was competitive with commercial products.

X-Ray Diffraction (XRD) Analysis

The XRD pattern shows the semicrystalline pattern of synthetic leather (Figure 2). The peaks of PVC appeared at the diffraction angles (2θ) of 19° and 24° [35–37]. The peak at 24° for the silica-modified composite was not observed clearly due to an overlap with the characteristic peak of silica at 22° [38,39]. This overlap peak reveals that the synthetic leather sample had been successfully modified with silica as a filler.

Table 3. Comparison of physical properties of composite and commercial products.

Material	Maximum Tensile Force (N)	Elongation (%)	Maximum Tear Force (N)	Adhesive Resistance (N)
S-60	410.74	16.70	57.91	18.17
Product X	163.67	17.49	51.81	34.18
Product Y	77.44	14.64	34.16	20.52

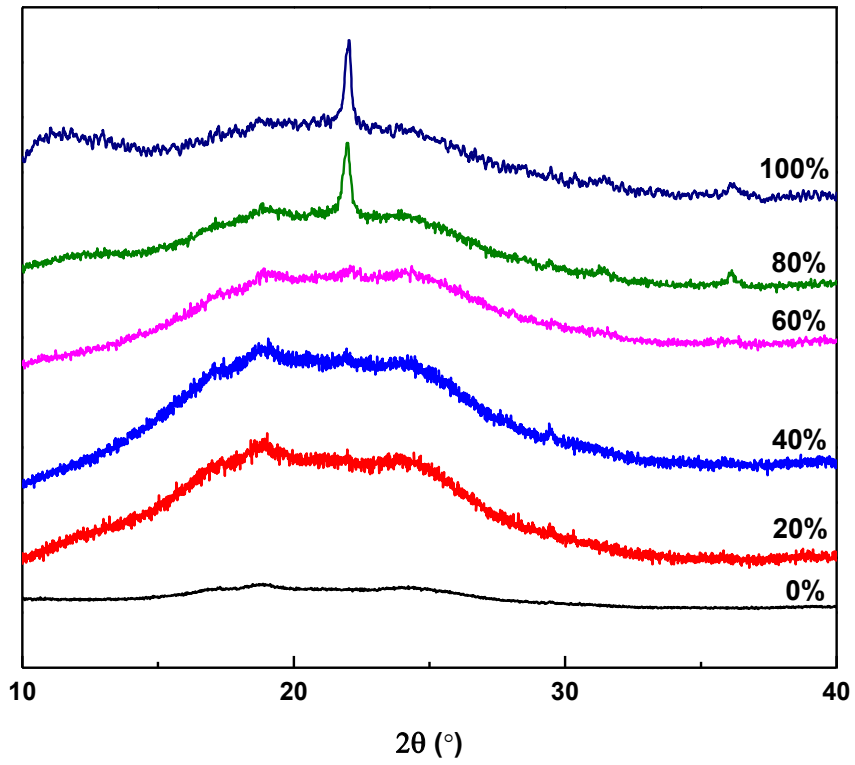

Figure 2. XRD patterns of the synthetic leather samples.

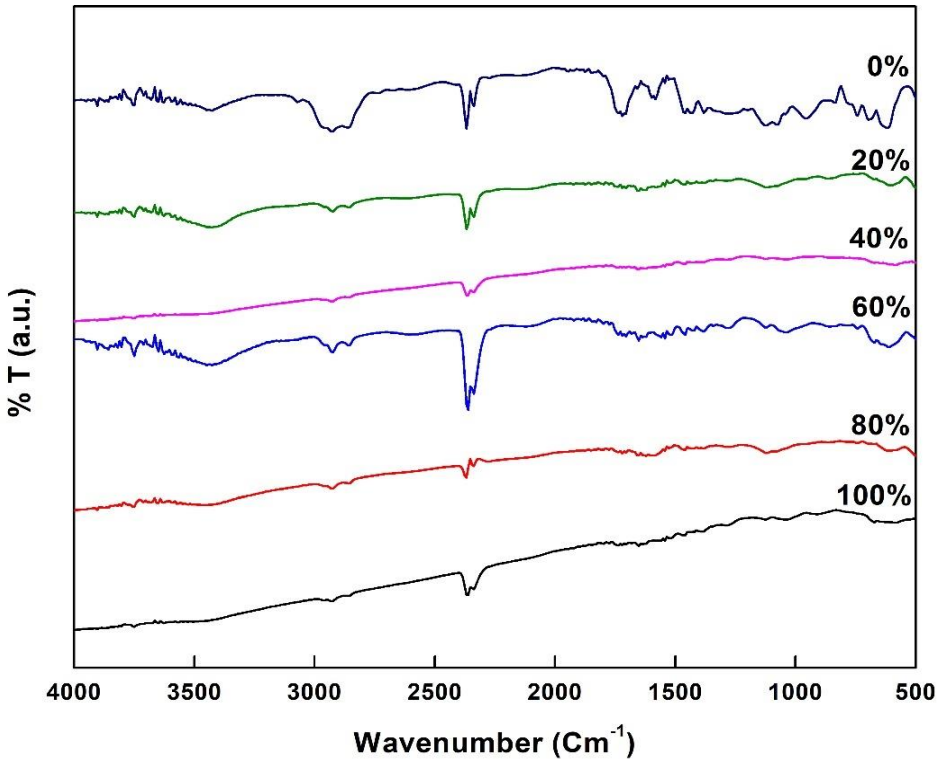

Figure 3. Infrared spectra of the synthetic leather samples.

Fourier Transform Infrared (FTIR) Analysis

The FTIR spectra indicated the successful modification of PVC using silica-based sugarcane bagasse ash filler (Figure 3). The absorption bands of PVC were observed at 617, 694, and 833 cm^{-1}, corresponding to the stretching vibration of C-Cl [40–42]. Additionally, the presence of Cl in PVC resulted in the absorption band at 1427 cm^{-1}, attributed to the symmetrical stretching vibration of CH_2-Cl. The bending and stretching vibrations of C-H were seen at 960 and 1273 cm^{-1}, respectively [42, 43]. The band around 1200 cm^{-1} overlapped with the stretching vibrations of a methylene group (-CH_2-), a methyl group (-CH_3), and CH-Cl [44]. The absorption band of C-H, an asymmetrical stretching vibration of CH_2, was also found at 2924 cm^{-1} [45, 46].

The interaction of PVC with DOP and epoxy resulted in the absorption bands at 1073 and 1126 cm^{-1}, due to C-O stretching. Likewise, the band at 1721 cm^{-1} due to C=O stretching revealed their interaction [40, 44]. The presence of silica was indicated by a band at 1073 cm^{-1} corresponding to the Si–O–Si group, which overlapped with the C–O band [9]. Additionally, a hydrogen bond was detected at 3426 cm^{-1}, as -OH stretching [46].

A change in absorption occurred after with the addition of silica as a filler. The intensity of the C-Cl absorption band decreased at around 620-700 cm^{-1}. A weaker intensity was also noted in the C-H peak at 2900 cm^{-1}. This is due to the decrease in the intermolecular interactions of PVC which were replaced by interactions between PVC and silica. These interactions are formed through hydrogen bonding between the hydrogen (H) of PVC and the oxygen (O) of the silanol group. Thus, the absorption intensity at 3400 cm^{-1} is dependent on the amount of hydrogen bonds formed.

Scanning Electron Microscopy and Energy Dispersive X-Ray (SEM-EDX) Analysis

The cross-sectional and surface SEM images of the synthetic leather samples are shown in Figure 4. The analysis was conducted on samples S-0, S-60, and product X as a comparison.

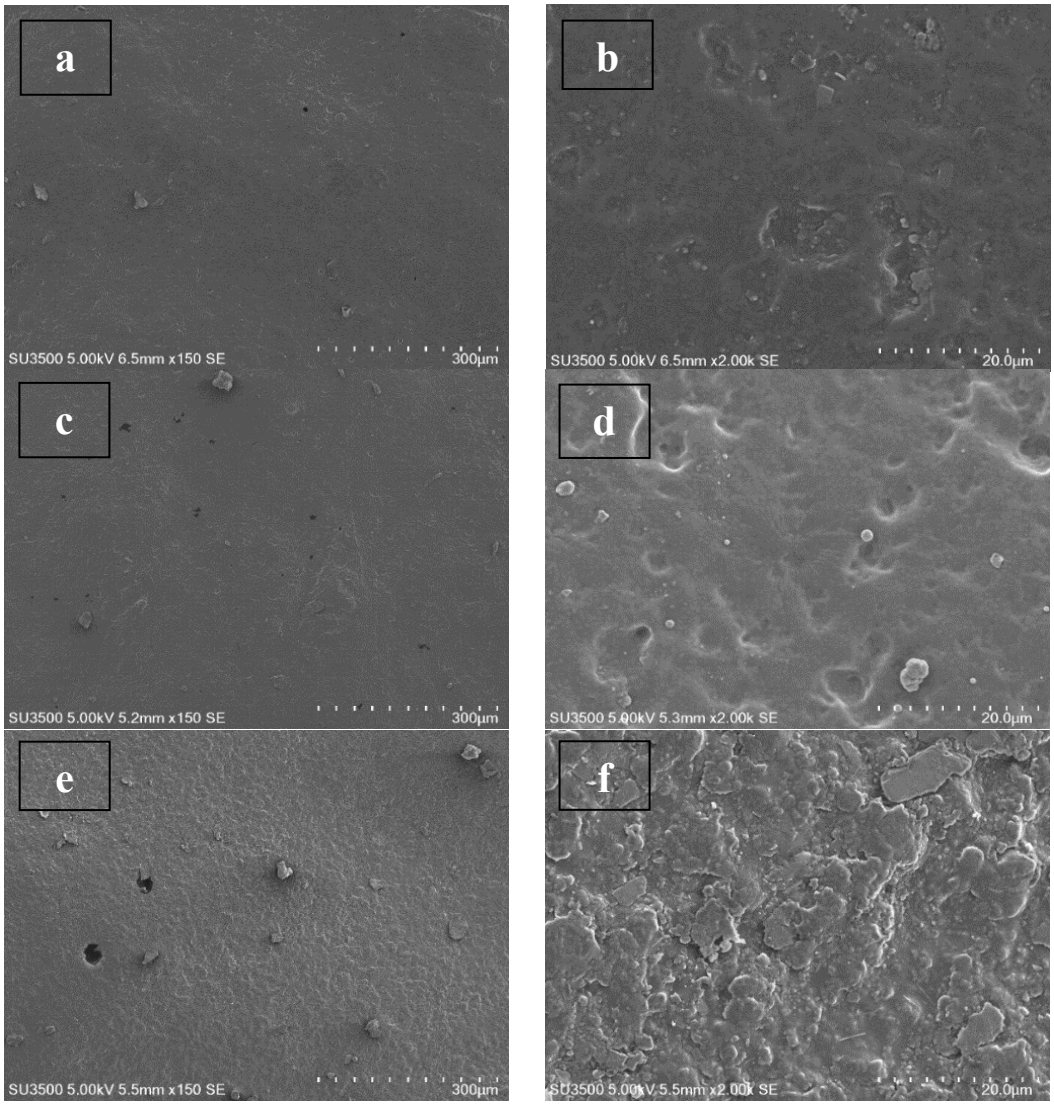

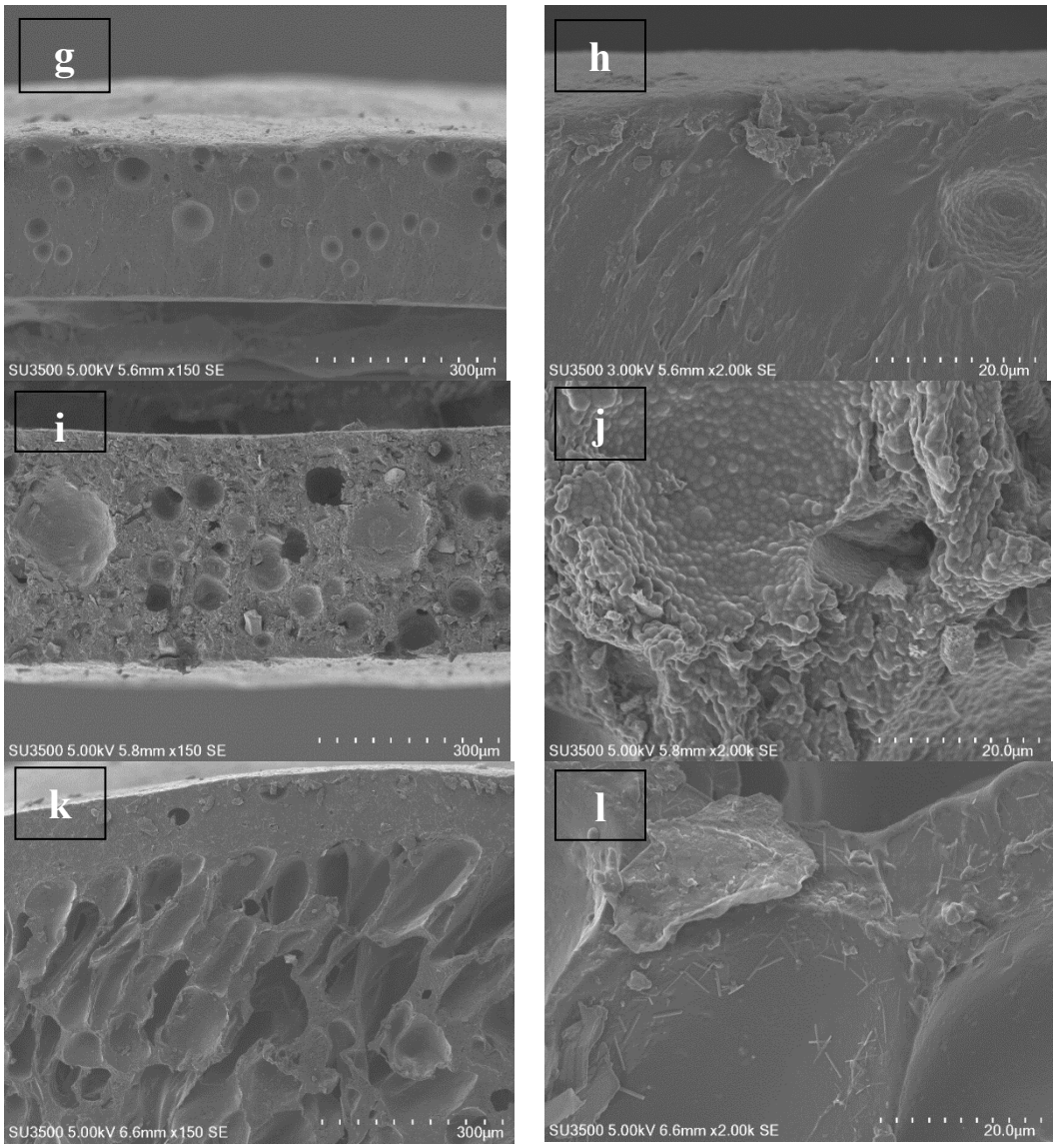

Figure 4. SEM surface images of synthetic leather samples at different magnifications: (a) S-0 (150x), (b) S-0 (2000x), (c) S-60 (150x), (d) S-60 (2000x), (e) Product X (150x), (f) Product X (2000x); and cross-sectional images: (g) S-0 (150x), (h) S-0 (2000x), (i) S-60 (150x), (j) S-60 (2000x), (k) Product X (150x), (l) Product X (2000x).

The SEM images show that the addition of a filler affected the surface of the composite. This is observed in Figure 4, where S-60 had a bumpy surface, while the surface of S-0 was less bumpy. When compared to product X, S-60 had fewer lumps and less roughness, indicating a more uniform structure. The cross-sectional images in Figure 4 show the dominant holes in product X. This is caused by the foaming agent that is commonly added to synthetic leather composites to prevent stretching or wrinkling. The foaming agent produces a foamy plastic structure that is softer and has a low density. Several holes were also found in S-60, indicating that SBA can provide a blowing agent-like effect, which was not found in S-0.

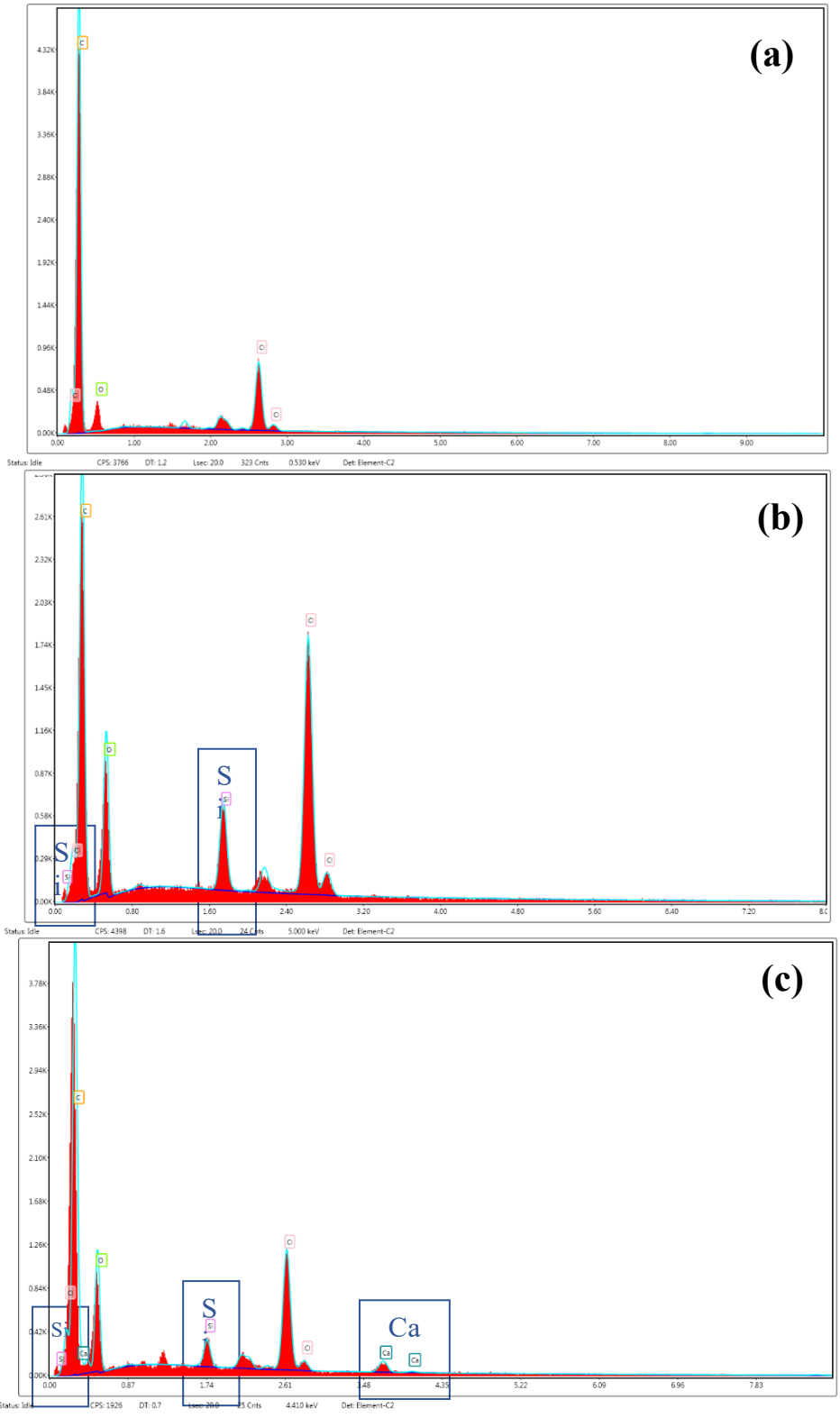

Figure 5. EDS spectra of the synthetic leather samples: (a) S-0, (b) S-60, and (c) Product X.

The EDX (Energy dispersive X-ray) spectra in Figure 5 show the presence of Si and O elements indicative of silica in S-60, while this was not detected in the spectra of S-0. The results confirm the presence of a Si-containing filler in the synthetic leather samples. In addition, silica and calcium were observed in the EDX spectra of product X, indicating that it also contained silica and calcium as fillers.

Table 4. Thermal degradation data of the synthetic leather and commercial samples.

Material	First stage		Second stage		Third stage		Total weight loss (%)
	Temp. (°C)	Weight loss (%)	Temp. (°C)	Weight loss (%)	Temp. (°C)	Weight loss (%)	
S-0	255.07	38.639	293.48	36.069	466.05	18.927	94.012
S-20	219.98	20.678	306.12	32.494	463.35	16.767	86.260
S-40	216.74	34.854	301.82	29.805	463.89	14.676	80.054
S-60	216.20	20.886	302.35	39.451	463.36	13.699	75.196
S-80	224.82	22.609	292.66	36.722	464.43	11.905	72.650
S-100	224.27	24.991	288.89	31.528	464.96	11.400	69.571
Product X	220.45	32.659	272.37	27.207	470.37	15.320	78.589
Product Y	215.13	29.097	291.58	27.221	439.15	26.905	85.752

Thermal Analysis

The TGA (Thermal Gravimetric Analysis) data are displayed in Table 4. Based on these results, the samples underwent three stages of thermal degradation. The first stage was the initial shoulder at about 216-255 °C. This is ascribed to the early onset PVC dehydrochlorination [47–49]. The temperature range in the second stage was around 288-306 °C, attributed to a major degradation step corresponding to extensive HCl release from PVC [47–49]. The third decomposition occurred at 463-466 °C, and was due to the degradation of conjugated polyene sequences and subsequent char formation [48–50].

The total weight loss decreased as silica concentration increased, indicating improved thermal stability. Furthermore, the weight loss of the composite samples fell within the typical range for commercial products (Table 4), confirming comparable thermal stability.

CONCLUSION

In this study, SBA was used as a filler for synthetic leather. The physical and thermal analyses showed that optimal properties were obtained with S-60. This material had the highest tensile and tear force values, at 410.74 N and 57.91 N, respectively. It was also thermally stable, with a total weight loss of 75.196%. Based on our comparison, the synthetic leather samples produced in this study, especially S-60, showed properties comparable to the commercial samples.

ACKNOWLEDGEMENTS

This work was supported by the Industry Learning Centre, Indonesian Ministry of Industry, through the *Sarana Penelitian Industri Terapan* (SPIRIT) Grant 2018. We are deeply grateful to Professor Katja Loos from the Macromolecular Chemistry & New Polymeric Materials research group, University of Groningen, The Netherlands, for her generous support in granting permission to perform the TGA analyses. We are also grateful to Jur van Dijken for his valuable support with the TGA. We sincerely appreciate Tijn C. de Leeuw for his helpful feedback on the manuscript.

REFERENCES

1. Mohamed, O. A., Abd-El-All, A. S., Masoud, R. A. and ElSayed, H. (2021) Activity of inorganic salts on different properties of synthetic leather. *Egypt. J. Chem.*, **64**, 3971–3979.

2. Mazitova, A. K., Zaripov, I. I., Aminova, G. K., Ovod, M. V. and Suntsova, N. L. (2022) Fillers for polymer composite materials. *Nanotechnologies in Construction*, **14**, 294–299.

3. Ramesh, M., Rajeshkumar, L. N., Srinivasan, N., Kumar, D. V. and Balaji, D. (2022) Influence of filler material on properties of fiber-reinforced polymer composites: A review. *E-Polymers*, **22**, 898–916.

4. Bokobza, L. (2023) Elastomer Nanocomposites: Effect of Filler–Matrix and Filler–Filler Interactions. *Polymers (Basel)*, **15(2900)**, 1–22.

5. Afgan, S., Ullah, N., Sulaiman, M., Ali, I., Iqbal, T., Younas, M. and Rezakazemi, M. (2022) High strength insulating polymeric composite based on recycled/virgin polyethylene terephthalate (PET) reinforced with hydrous magnesium silicate (talc). *Journal of Materials Research and Technology*, **21**, 3579–3593.

6. Sourprae, K., Kalkornsurapranee, E., Lehman, N., Chuaybamrung, A., Tuljittraporn, A., Nakaramontri, Y., Krainoi, A., Johns, J., Songtipya, L. and Uthaipan, N. (2022) Leather-Like Material Based on Natural Rubber Composites. *Journal of Physical Science*, **33**, 65–82.

7. Xia, Y., Yang, K., Feng, X. and Wang, Y. (2022) Tribological properties of modified kaolin doped polymer as polytetrafluoroethylene grease additive. *Tribol. Int.*, **173(107612)**, 1–12.

8. Zaripov, I. I., Vikhareva, I. N., Mazitova, K. A., Shevelev, I. N. and Mazitova, A. K. (2022) Influence of nanoadditives on PVC composition properties. *Nanotechnologies in Construction*, **14**, 205–210.

9. Zhang, S., Huang, Q., Chen, L., Zhong, Y., Hu, F., Wu, K., Yin, X., Hamza, M. F., Wei, Y. and Ning, S. (2024) Phosphination of amino-modified mesoporous silica for the selective separation of strontium. *J. Hazard. Mater.*, **467(133741)**, 1–12.

10. Abdollahi Boraei, S. B., Bakhshandeh, B., Mohammadzadeh, F., Haghighi, D. M. and Mohammadpour, Z. (2024) Clay-reinforced PVC composites and nanocomposites. *Heliyon*, **10(e29196)**, 1–21.

11. Yang, X., Du, G., Shuai, H., Xu, X. and Wang, J. (2025) Study on the Mechanical and Thermal Properties of Waterborne Polyurethane-Modified Aluminum Hydroxide and Its Application in LDPE Plastics. *Polymers (Basel)*, **17(556)**, 1–17.

12. Liang, C., Zheng, S., Chen, Z., Wei, S., Sun, Z. and Li, C. (2022) Study on surface modification of ground calcium carbonate with novel modifier and its PVC filling performance. *Powder Technol.*, **412(118028)**, 1–13.

13. Khoshnoud, P. and Abu-Zahra, N. (2018) Kinetics of thermal decomposition of PVC/fly ash composites. *International Journal of Polymer Analysis and Characterization*, **23**, 170–180.

14. Seroka, N. S., Taziwa, R. T. and Khotseng, L. (2022) Extraction and Synthesis of Silicon Nanoparticles (SiNPs) from Sugarcane Bagasse Ash: A Mini-Review. *Applied Sciences (Switzerland)*, **12(2310)**, 1–12.

15. Prabhath, N., Kumara, B. S., Vithanage, V., Samarathunga, A. I., Sewwandi, N., Maduwantha, K., Madusanka, M. and Koswattage, K. (2022) A Review on the Optimization of the Mechanical Properties of Sugarcane-Bagasse-Ash-Integrated Concretes. *Journal of Composites Science*, **6(283)**, 1–19.

16. Singh Rawat, S. and Sharma, A. (2023) Sugarcane bagasse ash—The future composite material: A literature review. *Mater. Today Proc.*

17. Castro, M. V. B. de S., Andrade, D. S. C. and Almeida, Y. M. B. (2025) Characterization and Evaluation of Sugarcane Bagasse Ash for Application as a Filler in Polymer Composites. *Revista de Gestão Social e Ambiental*, **19(e013523)**, 1–19.

18. Golewski, G. L. (2023) Mechanical properties and brittleness of concrete made by combined fly ash, silica fume and nanosilica with ordinary Portland cement. *AIMS Mater. Sci.*, **10**, 390–404.

19. Andrade Neto, J. da S., de França, M. J. S., Amorim Júnior, N. S. de and Ribeiro, D. V. (2021) Effects of adding sugarcane bagasse ash on the properties and durability of concrete. *Constr. Build. Mater.*, **266(120959)**, 1–13.

20. Farrant, W. E., Babafemi, A. J., Kolawole, J. T. and Panda, B. (2022) Influence of Sugarcane Bagasse Ash and Silica Fume on the Mechanical and Durability Properties of Concrete. *Materials*, **15**.

21. Abdalla, T. A., Koteng, D. O., Shitote, S. M. and Matallah, M. (2022) Mechanical Properties of Eco-friendly Concrete Made with Sugarcane Bagasse Ash. *Civil Engineering Journal (Iran)*, **8**, 1227–1239.

22. Nurwahid, I. H., Dimonti, L. C. C., Dwiatmoko, A. A., Ha, J. M. and Yunarti, R. T. (2022) Investigation on SiO_2 derived from sugarcane bagasse ash and pumice stone as a catalyst support for silver metal in the 4-nitrophenol reduction reaction. *Inorg. Chem. Commun.*, **135(109098)**, 1–11.

23. Setyawan, N., Hoerudin, Harimurti, N. and Misgiyarta (2024) SiO_2 Content and Chemical Properties of Potassium Silicate Extracted from Sugarcane Bagasse Ash using Sol Technique. *IOP Conference Series: Earth and Environmental Science*, **1354(012015)**, 1–5.

24. Chuewangkam, N., Nachaithong, T., Chanlek, N., Thongbai, P. and Pinitsoontorn, S. (2022) Mechanical and Dielectric Properties of Fly Ash Geopolymer/Sugarcane Bagasse Ash Composites. *Polymers (Basel)*, **14**.

25. Chantit, F., El Abbassi, F. E. and Kchikach, A. (2022) Investigation on the reuse of the sugar co-products (Bagasse, Molasses, and Ash) as industrial wastes in the production of Compressed earth blocks. *Materials Today: Proceedings*, **58**, 1530–1534.

26. Kusuma, H. S., Permatasari, D., Umar, W. K. and Sharma, S. K. (2024) Sugarcane bagasse as an environmentally friendly composite material to face the sustainable development era. *Biomass Convers. Biorefin.*, **14**, 26693–26706.

27. Iqbal, M. A., Sahar, U. U., Bahrami, A., Yaseen, N. and Siddique, I. (2024) Development of Sugarcane Bagasse Ash Blended Cementitious Composites Reinforced with Carbon Nanotubes and Polypropylene Fibers. *Journal of Composites Science*, **8(94)**, 1–20.

28. Gupta, C. K., Sachan, A. K. and Kumar, R. (2021) Examination of Microstructure of Sugar Cane Bagasse Ash and Sugar Cane Bagasse Ash Blended Cement Mortar. *Sugar Tech.*, **23**, 651–660.

29. Goyal, P. K. and Murmu, M. (2024) A review of sugarcane bagasse ash: Characteristics, properties and sustainable applications in concrete. *IOP Conference Series: Earth and Environmental Science*, **1409(012002)**, 1–15.

30. Sousa, L. N., Figueiredo, P. F., França, S., de Moura Solar Silva, M. V., Borges, P. H. R. and da Silva Bezerra, A. C. (2022) Effect of Non-Calcined Sugarcane Bagasse Ash as an Alternative Precursor on the Properties of Alkali-Activated Pastes. *Molecules*, **27(1185)**, 1–18.

31. Chindaprasirt, P. and Rattanasak, U. (2020) Eco-production of silica from sugarcane bagasse ash for use as a photochromic pigment filler. *Sci. Rep.*, **10**.

32. Homavand, A., Cree, D. E. and Wilson, L. D. (2024) Polylactic Acid Composites Reinforced with Eggshell/$CaCO_3$ Filler Particles: A Review. *Waste*, **2**, 169–185.

33. Chung, K. -H. and Greener, E. H. (1990) Correlation between degree of conversion, filler concentration and mechanical properties of posterior composite resins, **17**.

34. Karakaya, N., Ersoy, O. G., Oral, M. A., Gonul, T. and Deniz, V. (2010) Effect of different fillers on physical, mechanical, and optical properties of styrenic-based thermoplastic elastomers. *Polym. Eng. Sci*., **50**, 677–688.

35. Sharaf, A., Elhady, M. A., Abdel-Galil, A., Eladl, S. M. and Nasr, A. (2023) Synthesis and characterization of gamma irradiated polyvinyl chloride/graphite carbon nitride nanocomposite films for electronic applications. *Journal of Thermoplastic Composite Materials*, **36**, 4841–4857.

36. Deraman, S. K., Tajuddin, N. A. and Hanibah, H. (2024) X-Ray Diffraction (XRD) and Surface Morphology Studies of PVC complexes Modified with Doping Salt and Additives. *Science Letters*, **18(2)**, 78–91.

37. Aberoumand, M., Soltanmohammadi, K., Rahmatabadi, D., Soleyman, E., Ghasemi, I., Baniassadi, M., Abrinia, K., Bodaghi, M. and Baghani, M. (2023) 4D Printing of Polyvinyl Chloride (PVC): A Detailed Analysis of Micro-structure, Programming, and Shape Memory Performance. *Macromol. Mater. Eng.*, **308**.

38. Haider, J. Bin., Haque, M. I., Hoque, M., Hossen, M. M., Mottakin, M., Khaleque, M. A., Johir, M. A. H., Zhou, J. L., Ahmed, M. B. and Zargar, M. (2022) Efficient extraction of silica from openly burned rice husk ash as adsorbent for dye removal. *J. Clean. Prod*., **380(135121)**, 1–11.

39. Draszewski, C. P., Silveira, N. M., Brondani, M., De Souza Cruz, A., Rezzadori, K., Mayer, F. D., Abaide, E. R., Mazutti, M. A., Tres, M. V. and Zabot, G. L. (2022) Use of Rice Husk Hydrolyzed by Subcritical Water to Obtain Silica from Agro-Industrial Waste. *Environ. Eng. Sci.*, **39**, 938–946.

40. Klempová, S., Oravec, M. and Vizárová, K. (2023) Analysis of thermally and UV–Vis aged plasticized PVC using UV–Vis, ATR-FTIR and Raman spectroscopy. *Spectrochim. Acta A Mol. Biomol. Spectrosc.*, **294**.

41. Li, W., Bai, Z., Zhang, T., Jia, Y., Hou, Y., Chen, J., Guo, Z., Kong, L., Bai, J. and Li, W. (2023) Comparative study on pyrolysis behaviors and chlorine release of pure PVC polymer and commercial PVC plastics. *Fuel*, **340(127555)**, 1–8.

42. Faiza, Khattak, A., Alahmadi, A. A., Ishida, H. and Ullah, N. (2023) Improved PVC/ZnO Nanocomposite Insulation for High Voltage and High Temperature Applications. *Sci. Rep.*, **13(7235)**, 1–15.

43. Su, W. W., Li, Y., Man, P. R., Sheng, Y. W. and Wang, J. (2025) Pyrolysis Kinetics and Gas Evolution of Flame-Retardant PVC and PE: A TG-FTIR-GC/MS Study. *Fire*, **8(262)**, 1–19.

44. Chen, J., Liu, Z., Jiang, J., Nie, X., Zhou, Y. and Murray, R. E. (2015) A novel biobased plasticizer of epoxidized cardanol glycidyl ether: synthesis and application in soft poly(vinyl chloride) films. *RSC Adv.,* **5**, 56171–56180.

45. Sui, D. P., Chen, H. X., Liu, L., Liu, M. X., Huang, C. C. and Fan, H. T. (2016) Ion-imprinted silica adsorbent modified diffusive gradients in thin

films technique: Tool for speciation analysis of free lead species. *Talanta*, **148**, 285–291.

46. Nuryono, Rosiati, N. M., Rettob, A. L., Suyanta, and Arryanto, Y. (2019) Coating of 2-aminobenzimidiazole and 1-(O-tolyl)biguanide functionalized silicas on iron sand magnetic material for sorption of $[AuCl_4]^-$. *Indonesian Journal of Chemistry*, **19**, 395–404

47. Jha, R. K., Neyhouse, B. J., Young, M. S., Fagnani, D. E. and McNeil, A. J. (2024) Revisiting poly(vinyl chloride) reactivity in the context of chemical recycling. *Chem. Sci.*, **15**, 5802–5813.

48. Čolnik, M., Kotnik, P., Knez, Ž. and Škerget, M. (2022) Degradation of Polyvinyl Chloride (PVC) Waste with Supercritical Water. *Processes*, **10(1940)**, 1-14.

49. Yang, S., Wang, Y. and Man, P. (2023) Kinetic Analysis of Thermal Decomposition of Polyvinyl Chloride at Various Oxygen Concentrations. *Fire*, **6(404)**, 1–15.

50. Hamza, M. and Shakoor, A. (2023) Thermogravimetric analysis for the characterization and comparative analysis of polyvinyl chloride (PVC) wall panel. *MATEC Web of Conferences*, **381(02008)**, 1–8.